Available online at www.sciencedirect.com
ScienceDirect
Ceramics International 38 (2012) 929–934
CERAMICS INTERNATIONAL
www.elsevier.com/locate/ceramint

Characterization of surface-modified montmorillonite nanocomposites

Aswini K. Mishra [a], Shaik Allauddin [a], Ramanuj Narayan [a], Tejraj M. Aminabhavi [b], K.V.S.N. Raju [a,*]

[a] Organic Coatings and Polymers Division, Indian Institute of Chemical Technology, Hyderabad, 500 007, India
[b] SET's College of Pharmacy, S.R. Nagar, Dharwad 580 002, India

Received 13 July 2011; received in revised form 5 August 2011; accepted 6 August 2011
Available online 11 August 2011

Abstract

Montmorillonite K-10 clay was surface-modified using the cationic surfactants viz., butyltriphenylphosphonium bromide (BTPB), cetyltrimethylammonium bromide (CTAB), and tributylhexadecylphosphonium (TBHPB) bromide. Of these, CTAB and TBHPB modified clays were chosen for surface grafting with 3-aminopropyltrimethoxy silane (APTMS) coupling agent. The nanocomposites were fully characterized by powder X-ray diffraction (XRD), solid state ^{29}Si NMR, Fourier transform infrared spectroscopy (FTIR) and thermogravimetry (TGA). The XRD and FTIR confirmed the increase in basal plane spacing and intercalation of long chain surfactant molecules into the clay gallery, while TGA indicated the onset degradation and 10% weight loss temperature ($T_{10\%}$) in case of quaternary phosphonium modified clay that was higher than the corresponding ammonium counterpart; these values increased further after the grafting with APTMS. The ^{29}Si NMR peak deconvolution study suggested that the molar % of *T* units and total degree of silica condensation for different APTMS grafted clay samples were more than 20% and 80%, respectively.

Keywords: K-10 clay; Surface grafting; Montmorillonite; APTMS

1. Introduction

Montmorillonite clay has high cation exchange/swelling capacity, high surface area, high porosity, and better surface activity [1], due to which it is a widely used adsorbent for treatment of toxic organic pollutants [2] in water purification and remediation of industrial wastes [3]. However, the intercalation of organic surfactants between clay galleries has an effect on their surface properties, which significantly increases the basal plane spacing [4]. The nanocomposites of modified clays are known to exhibit remarkable improvement in strength/heat resistance, decrease in gas permeability/flammability, and increase in biodegradability [5,6] compared to their untreated counterparts. These improvements are mainly due to the structural arrangement of organically modified clays and their interaction within the polymer matrix. Therefore, understanding of structural arrangements and degradation of organically modified clays is important before seeking their industrial applications.

Detailed degradation mechanism of various alkyl and arylammonium-modified clays has been reported elsewhere [7–9], suggesting that initial degradation starts with Hofmann elimination that depends on basicity of the anion, steric environment around ammonium ion and temperature [10]. However, the importance of phosphonium compounds in polymer-layered silicate nanocomposites is due to their ability to enhance thermal and flammability properties of the hybrid nanocomposites, which enable their use as flame retardants in textiles and paper industries, stabilizing agents for polyacrylonitrile fibers, heat stabilizers for nylon, and condensation additives for organic dyes to produce wash-fast colors [11].

In the earlier literature, surface modification of organo-clays using organosilane coupling agents has been investigated [12] for silation of silica with hexamethyldisilazane (HMDS) over the temperature range of 150–450 °C to observe that major products are hexamethyldisiloxane and ammonia, with lesser amounts of nitrogen and methane. Braggs et al. [13], studied the electrochemical properties of kaolinite before and after modification with chlorodimethyloctadecylsilane. Sudholter et al. [14], modified the surface of silica gel with 3-aminopropylethoxysilane and characterized its surface by solid state NMR.

* Corresponding author. Tel.: +91 40 27193208; fax: +91 40 27193991.
E-mail address: drkvsnraju@gmail.com (K.V.S.N. Raju).

0272-8842/$36.00
doi:10.1016/j.ceramint.2011.08.012

However, only few reports are available on the effect of different types of cationic surfactants to improve the thermal properties of organo-clays and how their properties can be influenced by introducing APTMS coupling agents onto the organo-clay surface. The present study deals with the structural conformation, physico-chemical as well as thermal properties of different types of organo-clay modified and siloxane-grafted composites.

2. Experimental procedure

2.1. Materials

BTPB, TBHPB, APTMS, and untreated montmorillonite K-10 clay were all purchased from Aldrich, Milwaukee, WI; hydrochloric acid (HCl), CTAB and sulfur free toluene were procured from s.d. fine chemicals, Mumbai, India. The sample codes and chemical compositions of different surfactant-modified and siloxane-grafted K10 clays are summarized in Table 1.

2.2. Characterizations

Powder X-ray diffraction patterns of different organo-clays and siloxane-modified clays were recorded at different diffraction angles (2θ) using Siemens/D-5000 diffractometer with CuKα radiation (λ = 1.5406 Å). The solid state ^{29}Si CPMAS NMR spectra were recorded on a UNITY-400, Varian, (Switzerland) spectrometer connected with high wattage amplifier. FTIR spectrum of pristine, organically modified and siloxane-grafted K10 clay samples were obtained by KBr disc. Mid-FTIR spectra were taken using Thermo Nicolet Nexus 670 spectrometer by scanning each sample for 128 times with a resolution of 4 cm^{-1} in the range of 400–4000 cm^{-1}. TGA of pure K10 clay, different organically modified clays and siloxane-modified clays were obtained using TA Instruments Inc., taking approximately 10 mg of sample heated in a platinum crucible. The samples were scanned by Q500 high-resolution TGA instrument operating at ramp of 10 °C/min from ambient to 600 °C in a high purity flowing nitrogen atmosphere (80 cm^3/min).

2.3. Modification K-10 clay and their surface-grafting by APTMS

The detailed K10-clay modification process was discussed before [15] and grafting of APTMS onto organic-clay surface was achieved as per published reports [16,17].

Table 1
Sample codes and chemical compositions of surfactant-modified and siloxane-grafted K10 clays.

Sample code	Chemical composition of formulations
Pure-K10	Pure K10 clay
K10-CTAB	Pure K10 clay + CTAB
K10-BTPB	Pure K10 clay + BTPB
K10-TBHPB	Pure K10 clay + TBHPB
K10-CTAB-Si	Pure K10 clay + CTAB + APTMS
K10-TBHPB-Si	Pure K10 clay + TBHPB + APTMS

3. Results and discussion

3.1. Powder X-ray diffraction (XRD) analysis

The overlapped XRD spectra of pristine and organically modified montmorillonite K10 clays are displayed in Fig. 1. The peak at 13.5 Å (1.35 nm) corresponds to basal plane spacing of unmodified montmorillonite clay that was shifted to lower 2θ value after modification with cationic surfactants, indicating the intercalation of long chain cationic surfactants into the clay gallery. The extent of intercalation is highest for K10-TBHPB (d = 2.30 nm) and lowest in case of K10-CTAB (d = 1.81 nm), suggesting the monolayer type of arrangement for CTAB-modified samples and bilayer to pseudo trilayer or paraffin-type arrangements for BTPB and TBHPB-modified samples [18]. However, the monolayer arrangement in case of K10-CTAB suggests that a large portion of ammonium modifier is associated with the external surface of montmorillonite, while the bilayer to pseudo trilayer type of arrangements in case of phosphonium-modified samples suggests a considerable swelling of clay gallery; this was also reflected in their thermal behavior (to be discussed later).

3.2. Solid state ^{29}Si NMR study

Solid state ^{29}Si NMR spectra of pristine clay, different surfactant-modified and siloxane-grafted organo-clays are shown in Fig. 2(a), while their chemical shifts, deconvoluted peak areas and degree of condensation (Dc) data are given in Table 2. The Dc values of the nanocomposites provide information on the presence of different silicon environments in addition to their degree of organic functionalization. In condensed species, silicon atom of SiO_2 unit (present in K10-clay or organo-clay) connected with mono-, di-, tri- and tetra-substituted –O–Si groups are designated as Q^1, Q^2, Q^3, and Q^4,

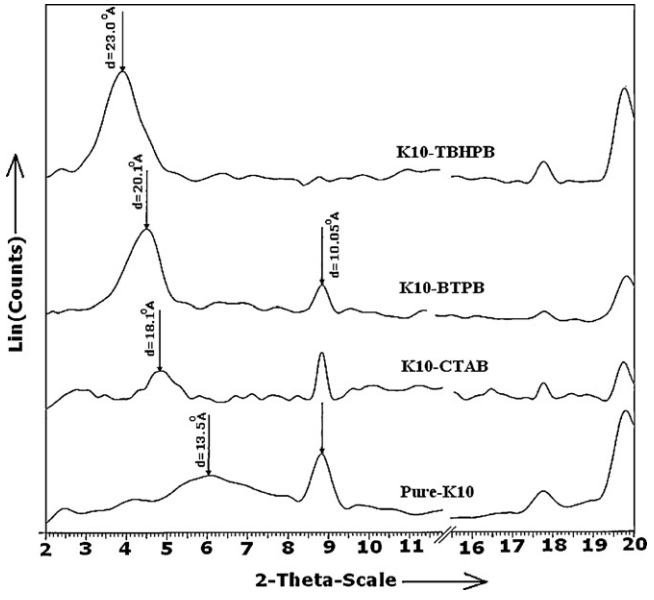

Fig. 1. XRD spectrum of pure K10 clay and organically modified K10-clays in 2θ range of 2–20.

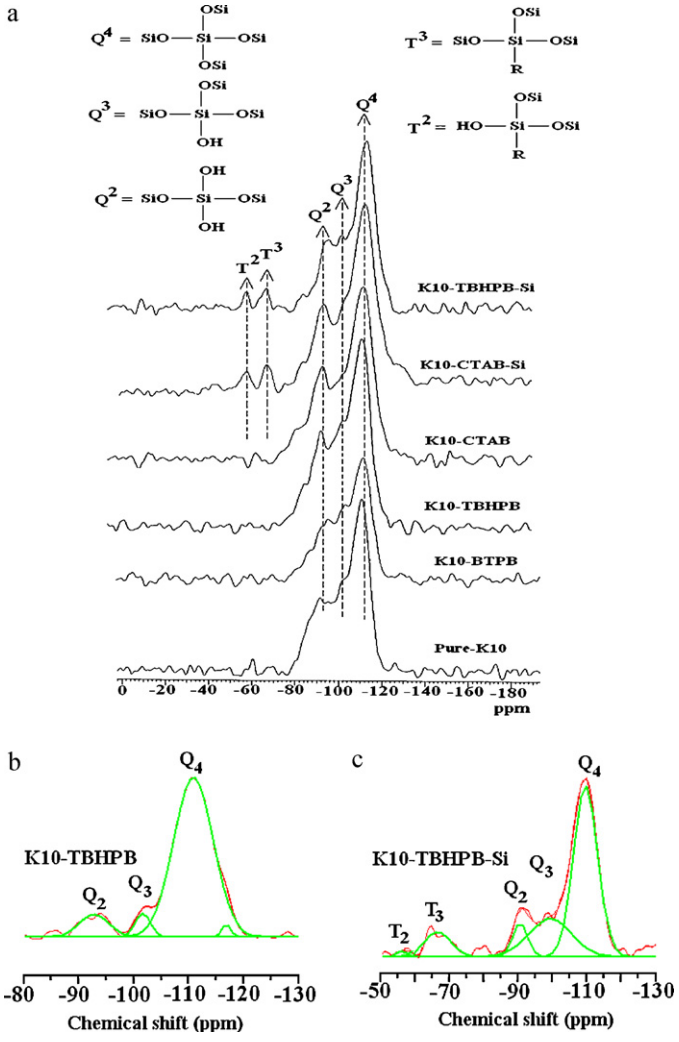

Fig. 2. (a) Solid state ^{29}Si NMR spectra of pure K10 clay along with organically modified and APTMS-grafted clays showing different Qi and Ti units. (b and c) Representative deconvulated solid state ^{29}Si CP/MAS NMR spectra of K10-TBHPB and K10-TBHPB-Si samples showing different Qi and Ti units.

respectively (shown in Scheme 1). On the other hand, silicon atom of APTMS connected with mono-, di-, and tri-substituted –O–Si groups are designated as T^1, T^2, and T^3, respectively [19]. The appearance of Q^2, Q^3 and Q^4 peaks between −91.2 to 92.5, −101.7 to 102.6 and −109.1 to 111.1 ppm in case of different organo-clays as well as APTMS-grafted organo-clays indicate the presence of $[(SiO)_2Si(OH)_2]$, $[Si(OSi)_3OH]$ and $[Si(OSi)_4]$ structural units, respectively [20].

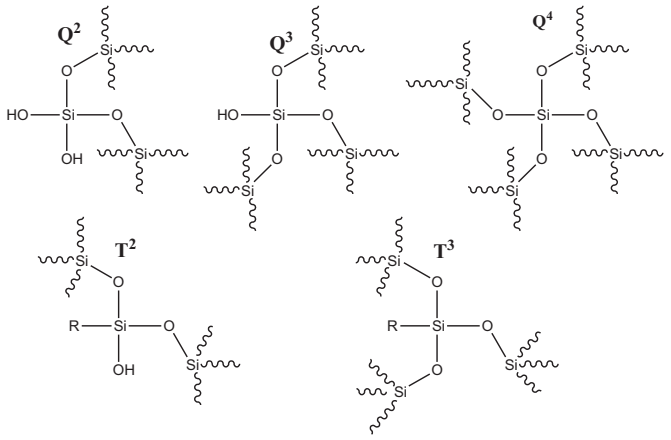

Scheme 1. The presence of different possible siloxane structural units in organic-clay and siloxane-modified samples.

It can be noticed that APTMS-grafted samples contain additional peaks T^2 and T^3 represented by $[Si(OSi)_2(OR')R]$ and $[Si(OSi)_3R]$ units between −58.3 to 59.4 and −64.7 to 65.1 ppm, which confirms the successful grafting of APTMS moiety onto organo-clay surface [21,22]. The decrease in intensity of Q^3 peaks and increase in intensity of Q^4 peaks as observed from the peak deconvolution area [see Table 2] indicates that probably interlayer surface silanol groups were modified by APTMS coupling agents forming more Q^4 units [20]. The different surfactant-modified organo-clays contain similar characteristic peaks as that of pure K10 clay, indicating that the microstructure of pure K10-clay was not altered even after the organic modification. The data presented in Table 2 suggests that the molar % of T units and total degree of silica condensation in case of different APTMS-grafted organo-clay samples are more than 20 and 80%, respectively. This indicates that *Dc* (%) for pure-K10 clay is higher than those of different surfactant-modified organo-clays and its value is highest for siloxane-grafted nanocomposites [see the deconvoluted peak areas shown in Fig. 2(b) and (c)].

3.3. FTIR analysis

FTIR absorption peak values for pristine K-10 clay, organically modified and siloxane-grafted organo-clays given in Table 3 confirm their structures as well as successful modification and APTMS grafting reactions. The absorption band at 3630 cm^{-1} is assigned to stretching vibrations of Al–OH

Table 2
Chemical shifts and relative proportions of different Ti and Qi species present in pure, surfactant modified and siloxane grafted *o*-clays calculated from ^{29}Si CP/MAS NMR spectra.

Sample codes	Chemical shifts (ppm)					Proportions (%)					*Dc* (%)
	T^2	T^3	Q^2	Q^3	Q^4	T^2	T^3	Q^2	Q^3	Q^4	
Pure-K10	–	–	−91.9	−101.7	−111.1	–	–	8.14	2.08	49.55	55.2
K10-CTAB	–	–	−92.5	−101.6	−110.0	–	–	4.73	2.46	32.95	37.2
K10-TBHPB	–	–	−91.8	−102.2	−110.8	–	–	4.05	2.23	38.83	42,6
K10-CTAB-Si	−59.4	−64.7	−90.6	−101.3	−109.4	1.12	22.12	11.86	20.55	37.97	82.2
K10-TBHPB-Si	−58.3	−65.1	−90.1	−101.6	−109.1	2.31	11.86	7.51	21.75	58.03	91.5

Table 3
FTIR results of organo-clay-modified and silica-grafted nanocomposites.

Wavenumber (cm^{-1})	Stretching and bending vibration zone
3658–3630	Stretching vibrations due to the inner surface or inner Al(OH) groups
3445	Free hydroxyl stretching of clay
3450	Stretching vibration of the absorbed water
1636	H–O–H bending vibrations of the interlayer water molecules [22]
1499	Characteristic band due to quaternary ammonium group
1070	Si–O–Si stretching of clay or APTMS
1004 and 840	Al–Al–OH stretching and Al–Mg–OH hydroxyl bending vibrations of clay [25]
530 and 464	Si–O–Al and Si–O–Si bending vibrations [27]
970 and 536	Stretching of terminal Si–OH groups and Al–O–Si deformation signal
2921 and 2862	Asymmetric and symmetric C–H stretching vibration

groups between the tetrahedral and octahedral sheets, while a broad band at 3429 cm^{-1} and a sharp band at 1636 cm^{-1} are assigned to hydroxyl stretching and H–O–H bending vibrations, respectively of the free and interlayer water molecules on montmorillonite clay [23]. The free, H-bonded and non-bridging Si–OH groups recognized by a broad, sharp and medium intensity bands are observed at 3690, 3400–3200 and 915 cm^{-1}, respectively [24]. The absorption band at 970 cm^{-1} is due to the stretching of terminal Si–OH on the surface of silica particles [25]. The coordination bands at 1208 and 1015 cm^{-1} represent stretching of Si–O in Si–O–Si groups of tetrahedral sheet [26], while a large band at 1038 cm^{-1} and small bands at 915 and 840 cm^{-1} are assigned to Si–O stretching and Al–Al–OH and Al–Mg–OH (present on the edges of the clay platelets) hydroxyl bending vibrations, respectively. A partial condensation might have occurred by Si–O–Si asymmetric stretching mode at 1130–1100 cm^{-1} as well as Si–O–Si symmetric stretching vibration at 1120 cm^{-1}, and the symmetric Si–O–Si stretching mode observed at 870 cm^{-1}. The absorption peaks below 550 cm^{-1} are due to the in-plane vibrations of octahedral ions and their adjacent oxygen layers [27]. The peaks at 525 and 456 cm^{-1} are associated with Si–O–Al and Si–O–Si bending vibrations, respectively [23,28].

The retention of peaks at 3429, 3630, 915, 840 and 526 cm^{-1} in modified nanocomposites indicates that clay modification and siloxane grafting did not alter the inherent clay structure. Compared to the unmodified clay, different APTMS-grafted samples exhibit some extra peaks at 2930, 1490, 1330 and 1556 cm^{-1} along with a decrease in intensity of –OH stretching band at 3656 cm^{-1} [25]. The absorption bands at 970 and 536 cm^{-1} are assigned to the stretching of terminal Si–OH groups and Al–O–Si deformation signal becomes stronger in the spectra of silane-modified clay. These observations suggest

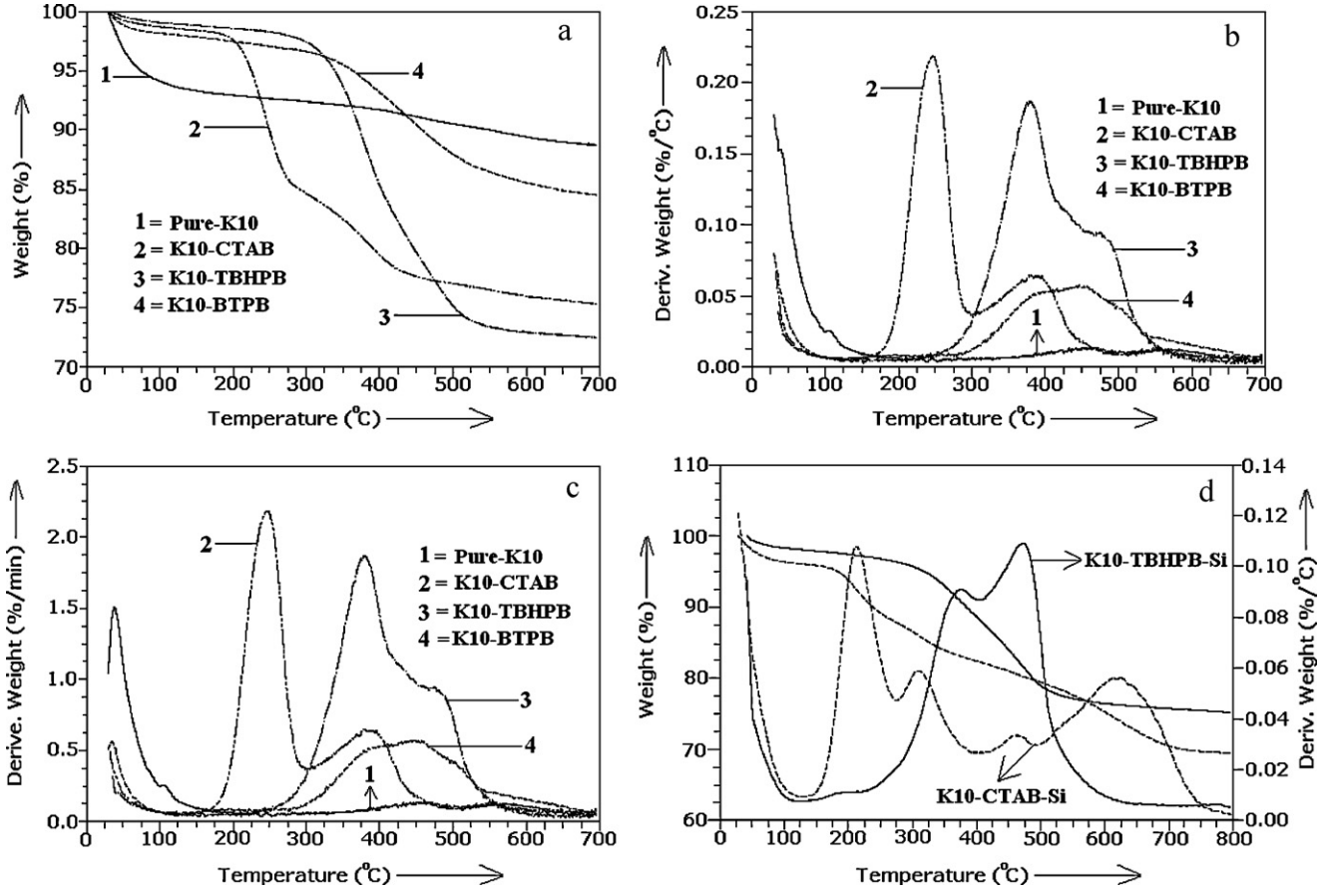

Fig. 3. (a–d) TG/DTA curves of pure K10-clay along with organically modified and siloxane-grafted clays.

Table 4
Thermal stability data of pristine, surfactant-modified and siloxane-grafted K10 clays.

Sample codes	T_{1ON}	T_{max}			$T_{10\%}$	% wt. remaining at 650 °C
		T_{1max}	T_{2max}	T_{3max}		
Pure-K10	385.3	456.7	566.4	–	543.8	88.9
K10-CTAB	194.1	246.3	389.2	554.4	249.3	75.6
K10-TBHPB	303.8	379.5	477.6	–	368.1	72.7
K10-BTPB	338.2	391.2	447.5	–	445.8	84.2
K10-CTAB-Si	177.5	212.8	308.6	462.1	240.2	72.4
K10-TBHPB-Si	295.4	374.2	473.1	–	379.3	76.1

the successful grafting of APTMS onto organo-clay surface as accompanied by the consumption of surface Al(OH) groups.

3.4. Thermogravimetric analysis

Thermal analysis technique has been quite useful to study the complex mineral systems and materials generated through modification of surfaces [29–31]. Thermal properties of different organically modified clays are related to the nature of surfactants used and their arrangements inside the interlayer space. In the present study, we have given more importance to the thermal property change by changing the type of organic modifier used during K10-clay modification and by introducing siloxane moieties onto the organo-clay surface. TG/DTA curves of pristine and organically modified clays are shown in Fig. 3(a–c), while that for different siloxane-grafted organo-clays are shown in Fig. 3(d) in the temperature ranges of 25–700 °C and 25–800 °C, respectively. Fig. 3(a) shows TGA profiles of pure and organically modified clays, which indicate a two-step decomposition profile with a very high char residue value for pure montmorillonite, while a three-step profile is observed for the organically modified clays. The decomposition step below 100 °C for all the samples is attributed to desorption of water molecules from the external surface as well as inside the clay gallery, while other steps between 200 and 600 °C corresponds to the decomposition of surfactant molecules [3,32,33]. Fig. 3(b) and (c) shows the derivatized thermograms of pristine and organo-clays vs. temp and time, respectively. The results show a three-step degradation profile for CTAB and two-step profile for BTPB and TBHPB-modified organo-clays, respectively.

Results reported in Table 4 suggest that the onset decomposition temperatures (T_{1ON}) and % wt. remaining at 650 °C for different phosphonium-modified clays are higher than those of ammonium-modified samples. For example, T_{1ON}, T_{1MAX} and $T_{10\%}$ for K10-BTPB, K10-TBHPB and K10-CTAB samples are 338.2, 303.8, 194.1; 391.2, 379.5, 246.3 and 445.8, 368.1, 249.3 °C, respectively. This could be due more hydrophilic nature and relatively looser arrangement of alkyl ammonium surfactants in the interlayer space of the clay compared to phosphonium compounds [18,34,35]. The total amount of organic modifier present within the organo-clay gallery was determined from the wt.% loss occurred between 200 and 500 °C, which was found to be 20.4, 24.5 and 9.5% for K10-CTAB, K10-TBHPB and K10-BTPB samples, respectively. The APTMS-grafted organo-clay samples [shown in Fig. 3(d)] exhibit three decomposition steps of which the first one occurs below 160 °C due to the elimination of adsorbed water and carbon dioxide molecules, while the second one between 160 and 380 °C corresponds to the decomposition of aminopropyl groups followed by a third rapid degradation step occurring above 380 °C [36,37].

4. Summary

This work deals with the surface grafting of organo-modified montmorillonite K-10 clay using cationic surfactants such as cetyltrimethylammonium bromide (CTAB), butyltriphenylphosphonium bromide (BTPB), tributylhexadecylphosphonium (TBHPB) bromide through ion exchange mechanism. The CTAB and TBHPB-modified organo-clays were surface functionalized using 3-aminopropyltrimethoxy silane (APTMS) coupling agent. From the XRD data, a peak value at 13.5Å (1.35 nm) corresponding to basal plane spacing of unmodified montmorillonite clay was shifted to lower 2θ value after modification with cationic surfactants, suggesting the successful intercalation of long chain cationic surfactants into the clay gallery. The extent of intercalation is highest for K10-TBHPB ($d = 2.30$ nm) and lowest in case of K10-CTAB ($d = 1.81$ nm). FTIR confirmed the presence of intercalating agents in the clay gallery and APTMS moieties are successfully attached to the organo-clay surface. TGA suggested that thermal stability of organo-clays modified by quaternary phosphonium-based surfactant is higher than the corresponding ammonium counterparts due to more hydrophilic nature and relatively looser arrangement of alkyl ammonium surfactants in the interlayer space than the phosphonium compounds. TGA also suggests that 10% weight loss temperature ($T_{10\%}$) for APTMS-grafted organo-clays is higher than the corresponding simple organo-clays due to the formation of more thermally stable Si–O–Si linkages in the matrix, which acts as a thermal insulator and mass transfer barrier for volatile compounds generated during degradation. ^{29}Si NMR of APTMS-grafted samples showed the presence of additional peaks T^2 and T^3 represented by $[Si(OSi)_2(OR')R]$ and $[Si(OSi)_3R]$ units, which confirmed the successful grafting of APTMS moiety onto organo-clay surface. The ^{29}Si NMR peak deconvolution data suggest that molar % of T units and total degree of silica condensation in case of different APTMS-grafted organo-clay samples are more than 20% and 80%, respectively.

Acknowledgments

Mr. A.K. Mishra thanks Council of Scientific and Industrial Research (CSIR, New Delhi, India) for awarding a research fellowship. Professor T.M. Aminabhavi thanks the Council of Scientific and Industrial Research [21/(0760)/09/EMR-II], New Delhi, India for awarding the Emeritus Scientist.

References

[1] Y. Xi, Z. Ding, H. He, R.L. Frost, Structure of organoclays—an X-ray diffraction and thermogravimetric analysis study, J. Colloid Interface Sci. 277 (2004) 116–120.
[2] C.S. Kim, D.M. Yates, P.J. Heanet, The layered sodium silicate magadiite: an analog to smectite for benzene sorption from water, Clays Clay Miner. 45 (1997) 881–885.
[3] O. Meincke, B. Hoffmann, C. Dietrich, C. Friedrich, Viscoelastic properties of polystyrene nanocomposites based on layered silicates, Macromol. Chem. Phys. 204 (2003) 823–830.
[4] S.A. Boyd, S. Shaobai, J.F. Lee, M.M. Mortland, Pentachlorophenol sorption by organo-clays, Clays Clay Miner. 36 (1988) 125–130.
[5] J.W. Gilman, Flammability and thermal stability studies of polymer layered-silicate (clay) nanocomposites, Appl. Clay. Sci. 15 (1999) 31–49.
[6] J. Temuujin, Ts. Jadambaa, G. Burmaa, Sh. Erdenechimeg, J. Amarsanaa, K.J.D. MacKenzie, Characterisation of acid activated montmorillonite clay from Tuulant (Mongolia), Ceram. Int. 30 (2004) 251–255.
[7] W. Xie, W.P. Pan, D. Hunter, R. Vaia, Thermal degradation chemistry of alkyl quaternary ammonium montmorillonite, Chem. Mater. 13 (2001) 2979–2990.
[8] J. Zhu, A.B. Morgan, F.J. Lamelas, C.A. Wilkie, Fire properties of polystyrene-clay nanocomposites, Chem. Mater. 13 (2001) 3774–3780.
[9] V. Hlavaty, V.S. Fajnor, Thermal stability of clay/organic intercalation complexes, J. Therm. Anal. Calorim. 67 (1) (2002) 113–118.
[10] F.G. Ramos Filho, T.J.A. Melo, M.S. Rabello, S.M.L. Silva, Thermal stability of nanocomposites based on polypropylene and bentonite, Polym. Degrad. Stab. 89 (2005) 383–392.
[11] G.M. Kosolapoff, L. Maier, Organic Phosphorus Compounds, vol. 2, John Wiley & Sons, New York, 1972.
[12] S.V. Slavov, A.R. Sanger, K.T. Chuang, Mechanism of silation of silica with hexamethyldisilazane, J. Phys. Chem. B 104 (2000) 983–989.
[13] B. Braggs, D. Fornasiero, J. Raltston, R.St. Smart, The effect of surface modification by an organosilane on the electrochemical properties of kaolinite, Clays. Clay. Miner. 42 (1994) 123–136.
[14] E.J.R. Sudholter, R. Huis, G.R. Hays, N.C.M. Alma, Solid-state silicon-29 and carbon-13 NMR spectroscopy using cross-polarization and magic-angle-spinning techniques to characterize 3-chloropropyl and 3-aminopropyl-modified silica gels, J. Colloid Interface Sci. 103 (1985) 554–560.
[15] D.K. Chattopadhyay, A.K. Mishra, B. Sreedhar, K.V.S.N. Raju, Thermal and viscoelastic properties of polyurethane-imide/clay hybrid coatings, Polym. Degrad. Stab. 91 (2006) 1837–1849.
[16] M. Sabzi, S.M. Mirabedini, J. Zohuriaan-Mehr, M. Atai, Surface modification of TiO_2 nano-particles with silane coupling agent and investigation of its effect on the properties of polyurethane composite coating, Prog. Org. Coat. 65 (2009) 222–228.
[17] A.K. Mishra, R. Narayan, T.M. Aminabhavi, S.K. Pradhan, K.V.S. N. Raju, Hyperbranched polyurethane-urea-imide/o-clay-silica hybrids: Synthesis and characterization, J. Appl. Polym. Sci., in press.
[18] C.B. Hedley, G. Yuan, B.K.G. Theng, Thermal analysis of montmorillonites modified with quaternary phosphonium and ammonium surfactants, Appl. Clay. Sci. 35 (2007) 180–188.
[19] R.H. Glaser, G.L. Wilkes, Structure property behaviour of polydimethylsiloxane and poly(tetramethylene oxide) modified TEOS based sol-gel materials, Polym. Bull. 19 (1988) 51–57.
[20] K. Isoda, K. Kuroda, M. Ogawa, Interlamellar grafting of (-methacryloxypropylsilyl groups on magadiite and copolymerization with methyl methacrylate, Chem. Mater. 12 (2000) 1702–1707.
[21] R. Joseph, S. Zhang, W.T. Ford, Structure and dynamics of a colloidal silica-poly(methyl methacrylate) composite by ^{13}C and ^{29}Si MAS NMR spectroscopy, Macromolecules 29 (1996) 1305–1312.
[22] N.N. Herrera, J.M. Letoffe, J.L. Putaux, L. David, E.B. Lami, Aqueous dispersions of silane-functionalized laponite clay platelets. A first step toward the elaboration of water-based polymer/clay nanocomposites, Langmuir 20 (2004) 1564–1571.
[23] J. Madejova, FTIR techniques in clay mineral studies, Vib. Spectrosc. 31 (2003) 1–10.
[24] D.L. Wood, E.M. Rabinovich, Study of alkoxide silica gels by infrared spectroscopy, Appl. Spectrosc. 43 (1989) 263–267.
[25] C.A. Capozzi, R.A. Condrate, L.D. Pye, R.P. Hapannowicz, Vibrational spectral/structural changes from the hydrolysis/polycondensation of methyl-modified silicates. IV. IR spectral comparisons from the tetramethoxysilane/methyItrimethoxysilane/diethoxydimethyIsilane system, Mater. Lett. 18 (1994) 349–352.
[26] E. Sabah, M.S. Celik, Interaction of pyridine derivatives with sepiolite, J. Colloid. Interface Sci. 251 (2002) 33–38.
[27] S.F. Wang, M.L. Lin, Y.N. Shieh, Y.R. Wang, S.J. Wang, Organic modification of synthesized clay-magadiite, Ceram. Int. 33 (2007) 681–685.
[28] X. Xu, Y. Ding, Z. Qian, F. Wang, B. Wen, H. Zhou, Degradation of poly(ethylene terephthalate)/clay nanocomposites during melt extrusion: effect of clay catalysis and chain extension, Polym. Degrad. Stab. 94 (2009) 113–123.
[29] R.L. Frost, Z. Ding, H.D. Ruan, Thermal analysis of goethite, J. Therm. Anal. Calorim. 71 (3) (2003) 783–797.
[30] R.L. Frost, E. Horvath, E. Mako, J. Kristof, T. Cseh, The effect of mechanochemical activation upon the intercalation of a high-defect kaolinite with formamide, J. Colloid Interface Sci. 265 (2003) 386–395.
[31] R.L. Frost, E. Horvath, E. Mako, J. Kristof, A. Redey, Slow transformation of mechanically dehydroxylated kaolinite to kaolinite—an aged mechanochemically activated formamide-intercalated kaolinite study, Thermochim. Acta 408 (2003) 103–113.
[32] W. Xie, Z. Gao, K. Liu, W. Pan, R. Vaia, D. Hunter, Thermal characterization of organically modified montmorillonite, Thermochim. Acta 367 (2001) 339–350.
[33] Y. Sun, Z. Zhang, C.P. Wong, Study on mono-dispersed nano-size silica by surface modification for underfill applications, J. Colloid Interface Sci. 292 (2005) 436–444.
[34] Y.F. Xi, Q. Zhou, R.L. Frost, H.P. He, Thermal stability of octadecyltrimethylammonium bromide modified montmorillonite organoclay, J. Colloid Interface Sci. 311 (2007) 347–353.
[35] S.I. Marras, A. Tsimpliaraki, I. Zuburtikudis, C. Panayiotou, Thermal and colloidal behavior of amine-treated clays: the role of amphiphilic organic cation concentration, J. Colloid Interface Sci. 315 (2007) 520–527.
[36] S.R. Culler, S. Naviroj, H. Ishida, J.L. Koenig, Analytical and spectroscopic investigation of the interaction of CO_2 with amine functional silane coupling agents on glass fibers, J. Colloid Interface Sci. 96 (1983) 69–79.
[37] K.P. Battjes, A.M. Barolo, P. Dreyfuss, New evidence related to reactions of aminated silane coupling agents with carbon dioxide, J. Adhes. Sci. Technol. 5 (10) (1991) 785–799.